 CMES, vol.2, no.2, pp.171-181, 2001

Coupling of BEM/FEM for Time Domain Structural-Acoustic Interaction Problems

S.T. Lie[1], Guoyou Yu, Z. Zhao[2]

Abstract: The BEM/FEM coupling procedure is applied to 2-D time domain structural-acoustic interaction problems. The acoustic domain for fluid or air is modeled by BEM scheme that is suitable for both finite and infinite domains, while the structure is modeled by FEM scheme. The input impact, which can be either plane waves or non-plane waves, can either be forces acting directly on the structural-acoustic system or be explosion sources. The far field or near field explosion sources which are difficult to be simulated by finite element modeling, can be simulated exactly by boundary element modeling as internal sources. In order to maintain the stability of the coupling procedure, the linear θ method is used in this study. Three examples have been studied to demonstrate the efficiency and accuracy of the proposed numerical procedure.

keyword: BEM/FEM coupling model, structural-acoustic interaction, linear θ method, stability, far field or near field explosion.

1 Introduction

Time domain fluid-structure interaction problems have attracted significant attentions over the past few decades [Mindlin and Bleich (1952), Soliman and DiMaggio (1983), O'Regan and DiMaggio (1990), Pinsky and Abbound (1990)]. The finite element method (FEM) is ideal for modeling finite structures, but for infinite domains, the artificial boundary reflection should be considered and treated carefully [Bettess and Bettess (1991)].

Mindlin and Bleich (1952) were amongst the first researchers to develop the early time plane wave approximation (PWA) for simulating the effect of the infinite fluid (acoustic) medium. The PWA method was applied by DiMaggio et al. (1981) and Hamdan and Dowling (1995) to submerged spherical and spheroidal shells. Geers (1969) developed an analytical method based on a virtual mass approximation (VMA) for the infinite acoustic medium. The method was validated by studying the elastic response of a cylindrical shell excited by a transient acoustic wave. The proposed method was compared with PWA described previously, and numerical results demonstrated its superior performance for late time behaviors and low frequencies. By superimposing PWA and VMA, Ranlet et al. (1977) used the doubly asymptotic approximation (DAA) to model the infinite fluid medium, while model analysis was employed for the structure. The doubly asymptotic approximation had proved to be accurate for both early and late time behaviors and had been used by Zilliacus (1983) to analyze the response of a submerged fluid-filled cylinder subject to an incident plane step wave. The above methods have been used only to step plane incident wave problems caused by far field explosions. For near field explosions that will cause neither step wave nor plane wave, or for arbitrary shape submerged structures, application of the above methods will become very difficult. For such kind of problems, the boundary element method can be used and will yield a better result than the above mentioned methods.

The boundary element method, which is suitable for both finite and infinite domains, has been successfully used to many engineering problems on acoustic during the past two decades [Tanaka et al. (1998), Chen and Liu (1998)]. However, most of them are in frequency domain. Although the amount of data for the discretized governing equation grows linearly with each time step, it is not so important today as the computer power has increased many folds during the past two decades. Therefore, it is not difficult now to use the direct time domain BEM in solving real problems. The stability problem which had prevented the application of the BEM in time domain problems [Mansur (1983)], has been overcome by

[1] Corresponding Author
[2] School of Civil & Structural Engineering, Nanyang Technology University, Nanyang Avenue, Singapore 639798. Tel: (65) 790 5284, Fax: (65)792 1650, E-mail:cstlie@ntu.edu.sg

the linear θ method which had been shown to improve the stability of the BEM scheme greatly [Yu et al. (1999)].

In this paper, the fluid or air is modeled by BE method and the structure is modeled by FE method. The numerical results from BEM/FEM coupling procedure are first verified by comparing with analytical results. The impact loads acting on the coupling system are simulated by direct inputs as it is widely used by finite element method, or by use of internal sources for explosions that can be satisfied automatically by the boundary element method formulations. Hence, the BEM/FEM coupling procedure is suitable for all the general case problems where the waves are not confined to plane waves only and the structure can be of any shape. Detail discussions for the recent development of BEM and BEM/FEM coupling in time domain analysis can be found in Beskos (1997).

Three numerical examples for 2-D problems with either circular or noncircular structure are analyzed in this paper to show the validity of the proposed method for structural-acoustic problems.

2 Acoustic boundary element method modeling

The governing equation for acoustic problem can be written as:

$$\nabla^2 p - \frac{1}{c^2}\ddot{p} = -\gamma(q,t) \tag{1}$$

where ∇^2 is the Laplacian operator; p is the transient fluid pressure; c is the sound speed; and $\ddot{p}$ is the second partial time derivative of p; $\gamma(q,t)$ is the space (q) and time (t) dependence of source density.

The boundary integration formulation for Eq. 1 can be written as [Mansur (1983)]:

$$\begin{aligned} c(S)\,p(S,t) = {} & \\ & \frac{\rho}{4\pi}\left[-\int_0^{t^+}\int_\Gamma p^*(Q,t;S,\tau)\,\ddot{u}_n(Q,\tau)\,d\Gamma(Q)\,d\tau \right. \\ & \left. + \int_0^{t^+}\int_\Gamma \ddot{u}_n^*(Q,t;S,\tau)\,p(Q,\tau)\,d\Gamma(Q)\,d\tau\right] \\ & + \frac{1}{4\pi}\int_0^{t^+}\int_\Omega p^*(q,t;S,\tau)\,\gamma(q,\tau)\,d\Omega(q)\,d\tau \end{aligned} \tag{2}$$

where $p^*(Q,t;S,\tau)$ is the so-called fundamental solution given by

$$p^*(Q,t;S,\tau) = \frac{2c}{\sqrt{c^2(t-\tau)^2 - r^2}} H\left[c(t-\tau) - r\right];$$

$\ddot{u}_n = -\frac{1}{\rho}\frac{\partial p}{\partial n}$ is the normal acceleration at the boundary; $\ddot{u}_n^* = -\frac{1}{\rho}\frac{\partial p^*}{\partial n}$; and n is the coordinate in the direction of the unit outward vector $\vec{n}$, normal to Γ at Q.

Considering a set of discrete points $Q_j, \quad j = 1,2,\cdots,J$ on the Γ boundary and also a set of discrete values of time $t_n, \quad n = 1,2,\cdots,N$. So $p(Q,t)$ and $\ddot{u}_n(Q,t)$ can be approximated using a set of interpolation functions as indicated below:

$$\begin{cases} p(Q,t) = \sum\limits_{j=1}^{J}\sum\limits_{m=1}^{N} \phi_p^m(t)\,\eta_j(Q)\,p_j^m \\ \ddot{u}_n(Q,t) = \sum\limits_{j=1}^{J}\sum\limits_{m=1}^{N} \phi_a^m(t)\,\varphi_j(Q)\,\ddot{u}_{n\,j}^{\,m} \end{cases} \tag{3}$$

where η_j and φ_j are, respectively, spatial interpolation functions related to p and $\ddot{u}_n$, corresponding to a boundary node Q_j. ϕ_p^m and ϕ_a^m are, respectively, time interpolation functions related to p and $\ddot{u}_n$, corresponding to a discrete time t_m. $p_j^m = p(Q_j,t_m)$ and $\ddot{u}_{n\,j}^{\,m} = \ddot{u}_n(Q_j,t_m)$.

In the linear θ method [Yu et al. (1999)], a different last time step $[t_n, \quad t_{n+\theta}]$ is used, instead of $[t_n, \quad t_{n+1}]$, where $t_{n+\theta} = t_n + \theta\Delta t$, $\theta \geq 1$. The only difference of the linear θ method with the well known Wilson θ method [Bathe and Wilson (1973)] is that, the linear θ method assumes that both acceleration and traction vary linearly within $[t_n, \quad t_{n+\theta}]$, while the Wilson θ method makes such an assumption only for acceleration. For linear θ method, responses at time t_{n+1} can be calculated from responses at $t_{n+\theta}$ by following the relationship:

$$\begin{cases} p_i^{n+1} = \dfrac{1}{\theta}p_i^{n+\theta} + \dfrac{\theta-1}{\theta}p_i^n \\ \ddot{u}_{n_i}^{n+1} = \dfrac{1}{\theta}\ddot{u}_{n_i}^{n+\theta} + \dfrac{\theta-1}{\theta}\ddot{u}_{n_i}^n \end{cases} \tag{4}$$

Unknowns $p_i^{n+\theta}$ and $\ddot{u}_{n_i}^{n+\theta}$ can be calculated from the following equation [Yu et al. (1999)]:

$$\begin{aligned} & 4\pi c(S_i)\,p_i^{n+\theta} + \sum_{j=1}^{J} H_{ij}^{(n+\theta)(n+\theta)}\,p_j^{n+\theta} - \\ & \sum_{j=1}^{J} G_{ij}^{(n+\theta)(n+\theta)}\,\ddot{u}_{n\,j}^{\,n+\theta} = \sum_{m=1}^{n}\sum_{j=1}^{J} G_{ij}^{(n+\theta)m}\,\ddot{u}_{n\,j}^{\,m} - \\ & \sum_{m=1}^{n}\sum_{j=1}^{J} H_{ij}^{(n+\theta)m}\,p_j^m + S_i^{n+\theta} \end{aligned} \tag{5}$$

where:

$$\begin{cases} H_{ij}^{(n+\theta)m} = \rho \int_\Gamma \dfrac{\partial r(S_i,Q)}{\partial n(Q)} \eta_j(Q) \times \\ \quad \int_0^{t_{n+\theta}} [\phi_u^m(\tau) B^*(Q,t_{n+\theta};S_i,\tau) \\ \quad + \dfrac{1}{c} \dfrac{d\phi_u^m(\tau)}{d\tau} p^*(Q,t_{n+\theta};S_i,\tau)\,] d\tau d\Gamma(Q) \\ G_{ij}^{(n+\theta)m} = -\rho \int_\Gamma \varphi_j(Q) \int_0^{t_{n+\theta}} \phi_p^m(\tau) \times \\ \quad p^*(Q,t_{n+\theta};S_i,\tau)\, d\tau d\Gamma(Q) \\ S_i^{n+\theta} = \int_\Omega \int_0^{t_{n+\theta}} p^*(q,t_{n+\theta};S_i,\tau)\, \gamma(q,\tau)\, d\tau d\Omega(q) \end{cases} \tag{6}$$

and

$$\begin{cases} H_{ij}^{(n+\theta)(n+\theta)} = \rho \int_\Gamma \dfrac{\partial r(S_i,Q)}{\partial n(Q)} \eta_j(Q) \times \\ \quad \int_0^{t_{n+\theta}} \Big[\phi_u^{n+\theta}(\tau) B^*(Q,t_{n+\theta};S_i,\tau) \\ \quad + \dfrac{1}{c} \dfrac{d\phi_u^{n+\theta}(\tau)}{d\tau} p^*(Q,t_{n+\theta};S_i,\tau)\,] d\tau d\Gamma(Q) \\ G_{ij}^{(n+\theta)(n+\theta)} = -\rho \int_\Gamma \varphi_j(Q) \int_0^{t_{n+\theta}} \phi_p^{n+\theta}(\tau) \times \\ \quad p^*(Q,t_{n+\theta};S_i,\tau)\, d\tau d\Gamma(Q) \end{cases} \tag{7}$$

where

$$B^*(Q,t;S,\tau) = \frac{2c\,[c(t-\tau)-r]}{\sqrt{\left[c^2(t-\tau)^2 - r^2\right]^3}} H[c(t-\tau)-r] \tag{8}$$

In order to couple the BEM with FEM equations originated from the Newmark method, Eq. 5 has to be modified in such a way that p^{n+1} *and* $\ddot{u}_n^{n+1}$ instead of $p^{n+\theta}$ *and* $\ddot{u}_n^{n+\theta}$ should appear explicitly. From Eq. 4, one can write:

$$\begin{cases} p_i^{n+\theta} = \theta p_i^{n+1} - (\theta-1) p_i^n \\ \ddot{u}_{n_i}^{n+\theta} = \theta \ddot{u}_{n_i}^{n+1} - (\theta-1) \ddot{u}_{n_i}^n \end{cases} \tag{9}$$

Substitution of Eq. 9 into Eq. 5 gives:

$$\begin{aligned} &\theta \left[4\pi c(S_i) + \sum_{j=1}^{J} H_{ij}^{(n+\theta)(n+\theta)} \right] p_j^{n+1} - \theta \sum_{j=1}^{J} G_{ij}^{(n+\theta)(n+\theta)} \ddot{u}_{n\,j}^{n+1} \\ &= (\theta-1) \left\{ \left[4\pi c(S_i) + \sum_{j=1}^{J} H_{ij}^{(n+\theta)(n+\theta)} \right] p_j^n \right. \\ &\left. - \sum_{j=1}^{J} G_{ij}^{(n+\theta)(n+\theta)} \ddot{u}_{n\,j}^n \right\} + \sum_{m=1}^{n} \sum_{j=1}^{J} G_{ij}^{(n+\theta)m} \ddot{u}_{n\,j}^m \\ &- \sum_{m=1}^{n} \sum_{j=1}^{J} H_{ij}^{(n+\theta)m} p_j^m + S_i^{n+\theta} \end{aligned} \tag{10}$$

Eq. 10 can be written in matrix form as:

$$\begin{aligned} &\theta(\mathbf{C}+\mathbf{H}(\theta))\,\mathbf{p}^{n+1} - \theta \mathbf{G}(\theta)\,\ddot{\mathbf{u}}_n^{n+1} = \\ &\quad (\theta-1)\left[(\mathbf{C}+\mathbf{H}(\theta))\,\mathbf{p}^n - \mathbf{G}(\theta)\,\ddot{\mathbf{u}}_n^n\right] + \\ &\quad \sum_{m=1}^{n} \mathbf{G}(\theta)^{n-m+1} \ddot{\mathbf{u}}_n^m - \sum_{m=1}^{n} \mathbf{H}(\theta)^{n-m+1} \mathbf{p}^m + \mathbf{S}^{n+\theta} \end{aligned} \tag{11}$$

After considering the prescribed boundary conditions, the following equation arises:

$$\begin{aligned} \mathbf{A}\mathbf{x}^{n+1} &= \mathbf{B}\mathbf{y}^{n+1} + (\theta-1)\left[(\mathbf{C}+\mathbf{H}(\theta))\,\mathbf{p}^n - \mathbf{G}(\theta)\,\ddot{\mathbf{u}}_n^n\right] \\ &\quad + \left[\sum_{m=1}^{n} \mathbf{G}(\theta)^{n-m+1} \ddot{\mathbf{u}}_n^m - \sum_{m=1}^{n} \mathbf{H}(\theta)^{n-m+1} \mathbf{p}^{n-m+1} \right] \\ &\quad + \mathbf{S}^{n+\theta} \end{aligned} \tag{12}$$

Boundary unknowns at time t_{n+1} can be calculated from Eq. 12, which can also be used in the coupled BEM/FEM procedure in the same way usually employed for the standard BEM formulation as will be discussed in the following sections.

It can be seen that if θ=1, Eq. 12 becomes the standard BEM equation [Mansur (1983)]. However, the present formulation is stable when linear flux time interpolation functions are employed, whereas the standard one fails in closed domain analyses.

3 Newmark algorithm for finite element method

Coupling BEM and FEM using, respectively, linear θ and Wilson θ methods is straightforward. Thus, only the coupling procedure with Newmark FEM scheme will be studied here.

The FEM dynamic equilibrium equation for undamped systems reads:

$$\mathbf{M}\ddot{\mathbf{u}} + \mathbf{K}\mathbf{u} = \mathbf{R}(t) \tag{13}$$

where $\boldsymbol{M}$ and $\boldsymbol{K}$ are, respectively, mass and stiffness matrices, $\ddot{\mathbf{u}}$ and $\mathbf{u}$ are, respectively, the acceleration vector and the displacement (potential) vector. $\mathbf{R}(t)$ is the nodal force vector.

In the Newmark scheme, one has the following approximations:

$$\dot{u}^{n+1} = \dot{u}^n + \left[(1-\delta)\,\ddot{u}^n + \delta\ddot{u}^{n+1}\right]\Delta t \tag{14}$$

$$u^{n+1} = u^n + \dot{u}^n\Delta t + \left[\left(\frac{1}{2}-\alpha\right)\ddot{u}^n + \alpha\ddot{u}^{n+1}\right]\Delta t^2 \tag{15}$$

Substitution of Eq. 15, with $\alpha = \frac{1}{4}$ *and* $\delta = \frac{1}{2}$, into Eq. 13, results in the following equation:

$$\mathbf{K}_{eff}^{n+1}\,\ddot{\mathbf{u}}^{n+1} = \mathbf{R}_{eff}^{n+1} \tag{16}$$

where

$$\mathbf{K}_{eff} = \mathbf{M} + \frac{\Delta t^2}{4}\mathbf{K} \tag{17}$$

and

$$\mathbf{R}_{eff}^{n+1} = \mathbf{R}^n - \mathbf{K}\left(u^n + \Delta t\,\dot{u}^n + \frac{\Delta t^2}{4}\ddot{u}^n\right) \tag{18}$$

4 BEM/FEM coupling procedure

In order to develop the coupling procedure, consider first the Ω domain of a continuous medium subdivided into two sub-domains Ω_{BE} *and* Ω_{FE} ($\Omega = \Omega_{BE} \cup \Omega_{FE}$) with a common interface Γ_i. The sub-domain Ω_{BE} is to be modeled by boundary elements and the sub-domain Ω_{FE} by finite elements, as shown in Fig. 1.

The system of Eqs. 12 and 16 must be rewritten in a more suitable way to provide a better understanding of the coupling procedure. Before presenting the new version of those systems of equations, it is necessary to explain the notation employed: the subscript 'o' is associate to nodes that do not belong to Γ_i, whereas the subscript 'i' is associated to nodes that belong to Γ_i, the subscript 'in' is associated to normal part of the variables for the nodes belong to Γ_i, and the subscript '$i\tau$' is associated to parallel part of the variables for the nodes belong to Γ_i.

Then, it follows that Eq. 12, applied to Ω_{BE}, can be rewritten as:

$$\begin{bmatrix} \mathbf{A_{oo}} & \mathbf{A_{oi}} \\ \mathbf{A_{io}} & \mathbf{A_{ii}} \end{bmatrix} \begin{Bmatrix} \mathbf{x_{Bo}}^{\mathbf{n+1}} \\ \mathbf{x_{Bi}}^{\mathbf{n+1}} \end{Bmatrix} = \begin{bmatrix} \mathbf{B_{oo}} & \mathbf{B_{oi}} \\ \mathbf{B_{io}} & \mathbf{B_{ii}} \end{bmatrix} \begin{Bmatrix} \mathbf{y_{Bo}}^{\mathbf{n+1}} \\ \mathbf{y_{Bi}}^{\mathbf{n+1}} \end{Bmatrix} + \begin{Bmatrix} \mathbf{r_{Bo}^n} \\ \mathbf{r_{Bi}^n} \end{Bmatrix} \tag{19}$$

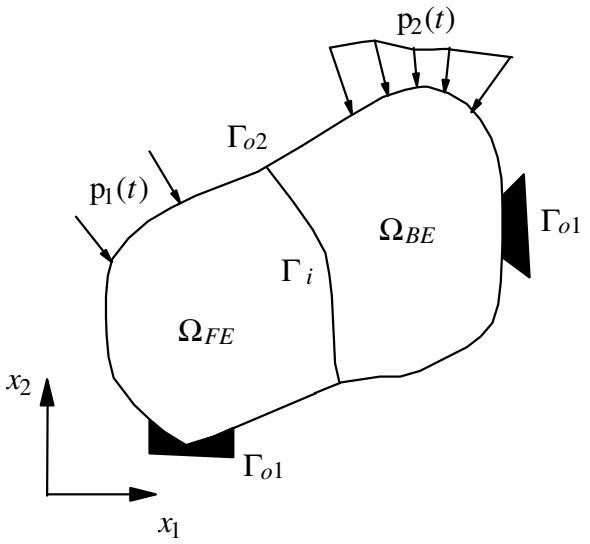

Γ_i - interface of FE and BE domains
Γ_{o1} - the boundary part where potential is prescribed
Γ_{o2} - the boundary part where flux is prescribed

Figure 1 : General representation of Ω_{FE} and Ω_{BE} subdomains

where $\mathbf{r_B^n} = \{\mathbf{r_{Bo}^n}, \mathbf{r_{Bi}^n}\}^T$ is obtained by reorganizing the vector $\mathbf{r_B^n}$ given by Eq. 20 below according to the interface of FE-BE domains. $\mathbf{r_B^n}$ is a known vector which accounts for u and p contributions up to the time t_n.

$$\mathbf{r'}_B^n = (\theta-1)\left[(\mathbf{C}+\mathbf{H}(\theta))\,\mathbf{p}^n - \mathbf{G}(\theta)\,\ddot{\mathbf{u}}^n\right] + \left[\sum_{m=1}^{n}\mathbf{G}(\theta)^{n-m+1}\,\ddot{\mathbf{u}}^m - \sum_{m=1}^{n}\mathbf{H}(\theta)^{n-m+1}\,\mathbf{p}^{n-m+1}\right] + \mathbf{S}^{n+\theta} \tag{20}$$

Eq. 16, by its turn, applied to Ω_{FE}, is rewritten as:

$$\begin{bmatrix} \tilde{\mathbf{K}}_{oo} & \tilde{\mathbf{K}}_{oi} \\ \tilde{\mathbf{K}}_{io} & \tilde{\mathbf{K}}_{ii} \end{bmatrix} \begin{Bmatrix} \tilde{\ddot{\mathbf{u}}}_{Fo}^{n+1} \\ \tilde{\ddot{\mathbf{u}}}_{Fi}^{n+1} \end{Bmatrix} = \begin{Bmatrix} \tilde{\mathbf{R}}_{Fo}^{n+1} \\ \tilde{\mathbf{R}}_{Fi}^{n+1} \end{Bmatrix} \tag{21}$$

$\tilde{\mathbf{K}}$ and $\tilde{\mathbf{R}}^{n+1}$ being obtained by adequate reorganization of $\mathbf{K}_{eff}$ and $\mathbf{R}_{eff}^{n+1}$ as respectively indicated by Eqs. 22 to 24 below:

$$\tilde{\mathbf{K}} = \begin{bmatrix} \tilde{\mathbf{K}}_{oo} & \tilde{\mathbf{K}}_{oi} \\ \tilde{\mathbf{K}}_{io} & \tilde{\mathbf{K}}_{ii} \end{bmatrix} = \begin{bmatrix} \mathbf{M}_{oo} + a_0\mathbf{K}_{oo} & \mathbf{M}_{oi} + a_0\mathbf{K}_{oi} \\ \mathbf{M}_{io} + a_0\mathbf{K}_{io} & \mathbf{M}_{ii} + a_0\mathbf{K}_{ii} \end{bmatrix} \tag{22}$$

$$\tilde{\mathbf{R}}^{n+1} = \left\{ \begin{array}{c} \tilde{\mathbf{R}}_{Fo}^{n+1} \\ \tilde{\mathbf{R}}_{Fi}^{n+1} \end{array} \right\} = \left\{ \begin{array}{c} \mathbf{R_{Fo}}^{n+1} \\ \mathbf{R_{Fi}}^{n+1} \end{array} \right\} + \left[\begin{array}{cc} \mathbf{K}_{oo} & \mathbf{K}_{oi} \\ \mathbf{K}_{io} & \mathbf{K}_{ii} \end{array} \right] \left\{ \begin{array}{c} \mathbf{r}_{Fo}^{n} \\ \mathbf{r}_{Fi}^{n} \end{array} \right\} \quad (23)$$

$$\left\{ \begin{array}{c} \mathbf{r}_{Fo}^{n} \\ \mathbf{r}_{Fi}^{n} \end{array} \right\} = \left\{ \begin{array}{c} a_0 \ddot{\mathbf{u}}_{Fo}^{n} + a_1 \dot{\mathbf{u}}_{Fo}^{n} + \mathbf{u}_{Fo}^{n} \\ a_0 \ddot{\mathbf{u}}_{Fi}^{n} + a_1 \dot{\mathbf{u}}_{Fi}^{n} + \mathbf{u}_{Fi}^{n} \end{array} \right\} \quad (24)$$

In Eqs. 22 and 24, the constants a_0 and a_1 are given by:

$$a_0 = \frac{\Delta t^2}{4} \quad \text{and} \quad a_1 = \frac{\Delta t}{4} \quad (25)$$

In order to derive the coupling procedure, the following coupling conditions on the interface should be considered:

i) equilibrium condition (for fluid-structure interaction problems only)

$$\mathbf{p}_{Fi}(s,t) = \mathbf{p}_{nFi}(s,t) = -\mathbf{p}_{Bi}(s,t) = -\mathbf{p}_{Bi}(s,t) \quad \text{for} \quad s \in \Gamma_i \quad (26)$$

ii) compatibility condition

$$\ddot{\mathbf{u}}_{nFi}(s,t) = \ddot{\mathbf{u}}_{nBi}(s,t) \qquad \text{for} \qquad s \in \Gamma_i \quad (27)$$

In order to reflect Eq. 26, Eq. 22 is modified as:

$$\left[\begin{array}{ccc} \tilde{\mathbf{K}}_{oo} & \tilde{\mathbf{K}}_{oi\tau} & \tilde{\mathbf{K}}_{oin} \\ \tilde{\mathbf{K}}_{ino} & \tilde{\mathbf{K}}_{inin} & \tilde{\mathbf{K}}_{ini\tau} \\ \tilde{\mathbf{K}}_{i\tau o} & \tilde{\mathbf{K}}_{i\tau in} & \tilde{\mathbf{K}}_{i\tau i\tau} \end{array} \right] \left\{ \begin{array}{c} \tilde{\ddot{\mathbf{u}}}_{Fo}^{n+1} \\ \tilde{\ddot{\mathbf{u}}}_{Fni}^{n+1} \\ \tilde{\ddot{\mathbf{u}}}_{Fn\tau}^{n+1} \end{array} \right\} = \left\{ \begin{array}{c} \tilde{\mathbf{R}}_{Fo}^{n+1} \\ \tilde{\mathbf{R}}_{Fni}^{n+1} \\ \tilde{\mathbf{R}}_{Fn\tau}^{n+1} \end{array} \right\} = \left\{ \begin{array}{c} \tilde{\mathbf{R}}_{Fo}^{n+1} \\ \tilde{\mathbf{R}}_{Fni}^{n+1} \\ \mathbf{0} \end{array} \right\} \quad (28)$$

$\tilde{\mathbf{R}}_{Fn\tau}^{n+1} = \mathbf{0}$ means that there is no interaction between fluid and structure at the tangent direction.

Bearing in mind that $\mathbf{x}_{Bi}^{n+1} = \mathbf{p}_{Bi}^{n+1}$, Eq. 19 can be written as:

$$\left\{ \begin{array}{c} \mathbf{x}_{Bo}^{n+1} \\ \mathbf{x}_{Bi}^{n+1} \end{array} \right\} = \left[\begin{array}{c} \mathbf{Q_{oo}} \left(\mathbf{B_{oo}} \mathbf{y}_{Bo}^{n+1} + \mathbf{r}_{Bo}^{n} \right) + \\ \mathbf{Q_{io}} \left(\mathbf{B_{oo}} \mathbf{y}_{Bo}^{n+1} + \mathbf{r}_{Bo}^{n} \right) + \\ \mathbf{Q_{oi}} \left(\mathbf{B_{io}} \mathbf{y}_{Bo}^{n+1} + \mathbf{r}_{Bi}^{n} \right) + \left(\mathbf{Q_{oo}} \mathbf{B_{oi}} + \mathbf{Q_{oi}} \mathbf{B_{ii}} \right) \mathbf{u}_{Bi}^{n+1} \\ \mathbf{Q_{ii}} \left(\mathbf{B_{io}} \mathbf{y}_{Bo}^{n+1} + \mathbf{r}_{Bi}^{n} \right) + \left(\mathbf{Q_{io}} \mathbf{B_{oi}} + \mathbf{Q_{ii}} \mathbf{B_{ii}} \right) \mathbf{u}_{Bi}^{n+1} \end{array} \right] \quad (29)$$

where

$$\left[\begin{array}{cc} \mathbf{Q}_{oo} & \mathbf{Q}_{oi} \\ \mathbf{Q}_{io} & \mathbf{Q}_{ii} \end{array} \right] = \left[\begin{array}{cc} \mathbf{A}_{oo} & \mathbf{A}_{oi} \\ \mathbf{A}_{io} & \mathbf{A}_{ii} \end{array} \right]^{-1} \quad (30)$$

The equivalent nodal load vector in FE formulations, related to tractions, is obtained from an integral of the type

$$\mathbf{R}_{Fin}(t) = \int_{\Gamma_i} \mathbf{H}^{\Gamma_i} \mathbf{p}_{Fin}(s,t)\, d\Gamma \quad (31)$$

corresponding to the whole interface of the coupling domain which consists of *nfei* finite elements. Thus the following equivalent nodal load vector at time t^{n+1} can be obtained:

$$\mathbf{R}_{Fin}^{n+1} = \sum_{e=1}^{nfei} \int_{\Gamma_e} \mathbf{H}^{\Gamma_e} \mathbf{p}_{Fin}(s,t_{n+1})\, d\Gamma \quad (32)$$

By considering the equilibrium condition in Eq. 26, it results:

$$\mathbf{R}_{Fin}^{n+1} = -\sum_{e=1}^{nfei} \int_{\Gamma_e} \mathbf{H}^{\Gamma_e} \mathbf{p}_{Bi}(s,t_{n+1})\, d\Gamma = -\left(\sum_{e=1}^{nfei} \int_{\Gamma_e} \mathbf{H}^{\Gamma_e} \gamma_e d\Gamma \right) \mathbf{p}_{Bi}^{n+1} = -\mathbf{F}\mathbf{x}_{Bi}^{n+1} \quad (33)$$

By considering the compatibility condition in Eq. 29 and then substituting the resulting expression for $\left\{ \mathbf{x}_{Bi}^{n+1} \right\}$ in Eq. 33, one has:

$$\mathbf{R}_{Fi}^{n+1} = -\mathbf{F}\left[\mathbf{Q}_{io} \left(\mathbf{B}_{oo} \mathbf{y}_{Bo}^{n+1} + \mathbf{r}_{Bo}^{n} \right) + \mathbf{Q}_{ii} \left(\mathbf{B}_{io} \mathbf{y}_{Bo}^{n+1} + \mathbf{r}_{Bi}^{n} \right) \right] - \mathbf{F}\left[\mathbf{Q}_{io}\mathbf{B}_{oi} + \mathbf{Q}_{ii}\mathbf{B}_{ii} \right] \ddot{\mathbf{u}}_{Fin}^{n+1} \quad (34)$$

With the above relation, it is possible to write the effective system of Eq. 28 as:

$$\left[\begin{array}{ccc} \tilde{\mathbf{K}}_{oo} & \tilde{\mathbf{K}}_{oi\tau} & \tilde{\mathbf{K}}_{oin} \\ \tilde{\mathbf{K}}_{\mathbf{ino}} & \tilde{\mathbf{K}}_{inin} + \mathbf{F}\left(\mathbf{Q}_{io}\mathbf{B}_{oi} + \mathbf{Q}_{ii}\mathbf{B}_{ii} \right) & \tilde{\mathbf{K}}_{ini\tau} \\ \tilde{\mathbf{K}}_{i\tau o} & \tilde{\mathbf{K}}_{i\tau in} & \tilde{\mathbf{K}}_{i\tau i\tau} \end{array} \right] \times \left\{ \begin{array}{c} \tilde{\ddot{\mathbf{u}}}_{Fo}^{n+1} \\ \tilde{\ddot{\mathbf{u}}}_{Fni}^{n+1} \\ \tilde{\ddot{\mathbf{u}}}_{Fn\tau}^{n+1} \end{array} \right\} = \left\{ \begin{array}{c} \tilde{\mathbf{R}}_{Fo}^{n+1} \\ \tilde{\mathbf{f}}_{Fni}^{n+1} \\ \mathbf{0} \end{array} \right\} \quad (35)$$

where

$$\tilde{\mathbf{f}}_{Fi}^{n+1} = \left(\mathbf{M}_{io}\mathbf{r}_{Fo}^{n} + \mathbf{M}_{ii}\mathbf{r}_{Fi}^{n} \right) - \mathbf{F}\left[\mathbf{Q}_{io} \left(\mathbf{B}_{oo} \mathbf{y}_{Bo}^{n+1} + \mathbf{r}_{Bo}^{n} \right) + \mathbf{Q}_{ii} \left(\mathbf{B}_{io} \mathbf{y}_{Bo}^{n+1} + \mathbf{r}_{Bi}^{n} \right) \right] \quad (36)$$

Displacements in the FE sub-domain can be obtained by solving Eq. 35. Other quantities such as velocities, accelerations, support reactions, stresses etc. in that subdomain can determined following standard procedures for FEM. By observing that $\ddot{\mathbf{u}}_{Bi}^{n+1} = \ddot{\mathbf{u}}_{Fin}^{n+1}$, it is also possible to calculate, by means of Eq. 29, the boundary unknowns in the region discretized with boundary elements and then the internal points state variables.

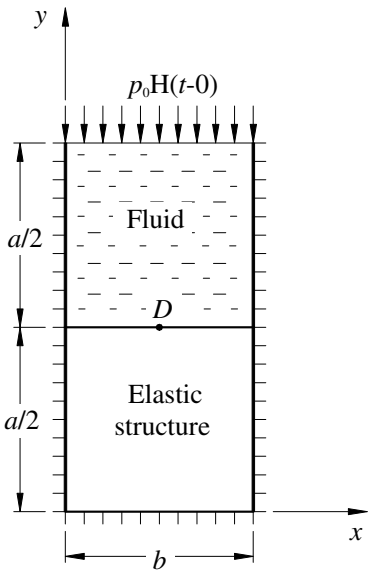

Figure 2 : One-dimensional fluid-structure system

5 Numerical examples

Three numerical examples are analyzed in this paper. The first has a finite fluid (acoustic) domain with external forces acting directly on the system, the second and the third have an infinite acoustic domain with far field or near field explosions respectively.

5.1 1-D fluid-structure interaction system

The first example is for a 1-D fluid-structure system, as shown in Fig. 2. The structure is fixed at the bottom and the fluid surface is subjected to a Heaviside-type forcing, $p_0 H(t-0)$. The Young's Modulus of the elastic structure is E, the Poisson's ratio ν=0, the mass density of the structure ρ_s is equal to that of the fluid ρ, the wave speed of the fluid $c = c_p = \sqrt{E/\rho_s}$, c_p is the compress wave speed for the structure. The displacements in x direction, u, are assumed to be zero at $x_1 = 0$ and $x_1 = b$ (a=2b) for any time t. As there is only displacement in y direction, it can be considered as 1-D fluid-structure interaction system. Since $c = c_p$, the results for the fluid-structure interaction system should be the same with that for a 1-D elastic rod [Mansur (1983)]. 32 finite elements are used to model elastic structure domain, 16 boundary elements with the same length L_j are used to model the fluid domain. Linear time interpolation is used for both displacement and stress in the BE formulation.

The numerical results, from the BEM/FEM coupling

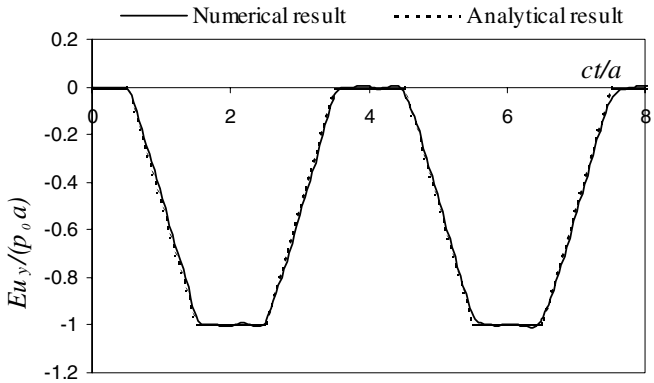

(a) Displacement

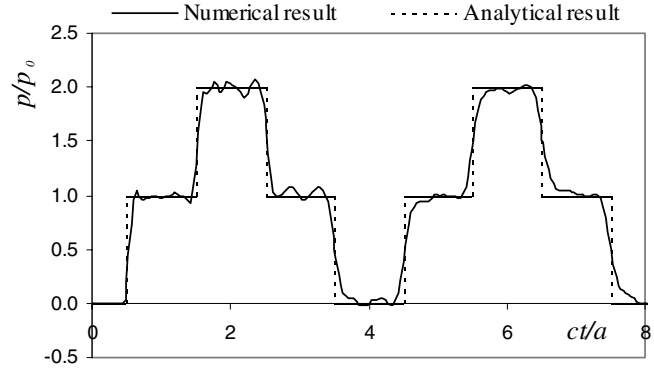

(b) Pressure

Figure 3 : Responses at point D in a one dimensional fluid-structure system $\Delta t = 0.3L_j/c, \theta = 1.4$

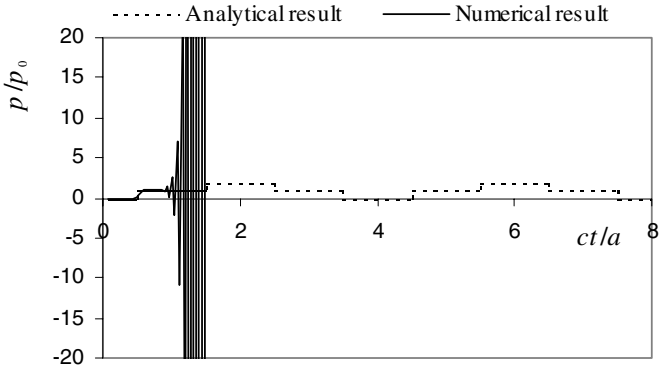

Figure 4 : Pressure at point D in a one dimensional fluid-structure system from standard BEM/FEM coupling procedure, $\Delta t = 0.3L_j/c$

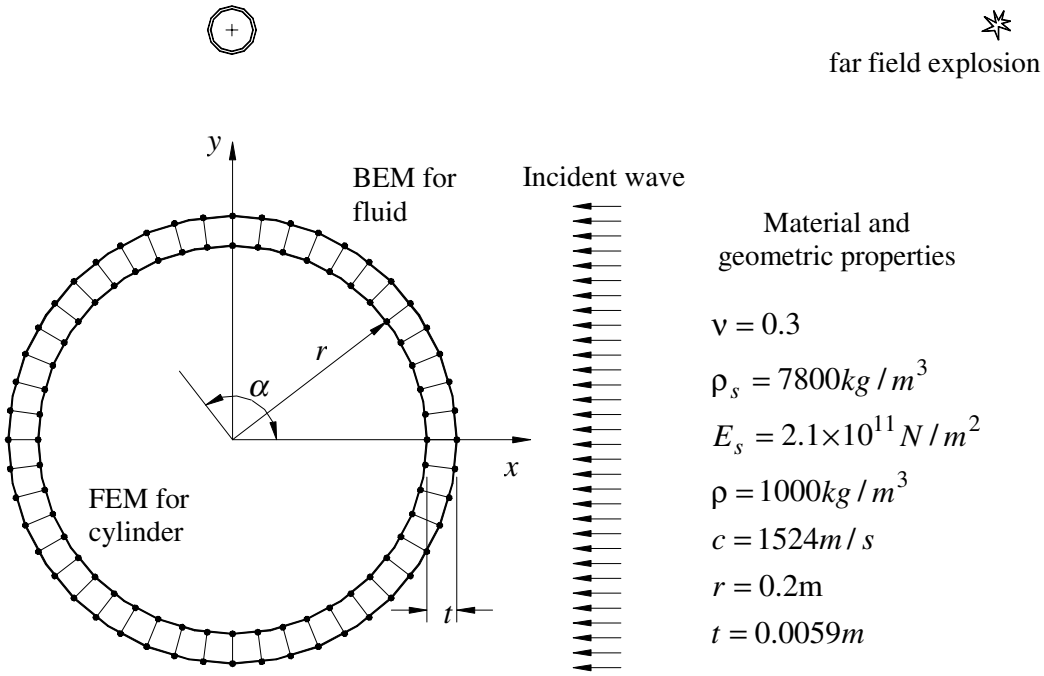

Figure 5 : Submerged cylinder subject to far field explosion

method, for the time histories of the vertical displacement and the fluid-structure pressure at point D are shown in Fig. 3, where the time step $\Delta t = 0.3L_j/c$. In order to get a stable result, the linear θ method [Yu et al. (1999)] is used in this example with θ=1.4. Comparing between the numerical and analytical results, one can see the feasibility of the BEM/FEM model for fluid-structure interaction problems.

It is noted that for the standard BEM/FEM coupling procedure (θ=1.0), a quick instability appears as shown in Fig. 4 for the fluid-structure pressure at point D. Which shows the necessity of using the linear θ method in time domain BEM/FEM coupling procedure.

5.2 *Cylinder submerged in water and subjected to an incident step wave*

This example is concerned for the interaction of an elastic infinite cylinder with an acoustic wave, caused by a series of far field explosions as shown in Fig. 5. The geometric and material properties of the cylinder and the fluid are also shown in Fig. 5. The far field explosions are chosen so that it will cause a nearly constant plane wave pressure in the free field (without cylinder) at the position where the cylinder is located. The reason for this is to compare the numerical results from the BEM/FEM procedure introduced here with the analytical solution given by Huang (1986), and reported by Zilliacus (1983) for a submerged cylinder subjected to a plane incident.

48 quadrilateral finite elements are used to model the cylinder and 48 boundary elements are used to model the infinite fluid. The normalized time step is chosen to be ΔT=$c\Delta t/r$=0.1, and the pressure is normalized by $P_0 = \rho c^2$.

Fig. 6 shows the normalized radial velocity of the cylinder (v_n) at different points on the outer surface, obtained from the BEM/FEM coupling procedure and from the analytical solution presented by Zilliacus (1983). The velocity was normalized with respect to the sound speed of the fluid medium, c, and the time was normalized with respect to r/c where r is the radius of the cylinder. Although the slight difference between the incident wave used here and that used by Zilliacus (1983) can give slight errors, the general trend for the results obtained by the proposed numerical procedure is reasonable.

5.3 *Dynamic response caused by air-explosion*

A typical civil engineering structure as shown in Fig. 7 subjected to an air explosion is analyzed with $E_s = 2.1\times10^{10}N/m^2$, $\rho_s = 2.6\times10^3 kg/m^2$, $\nu_s = 0.33$, $c_a = 340m/s$, $\rho_a = 1.3kg/m^3$. The subscript 's' represents

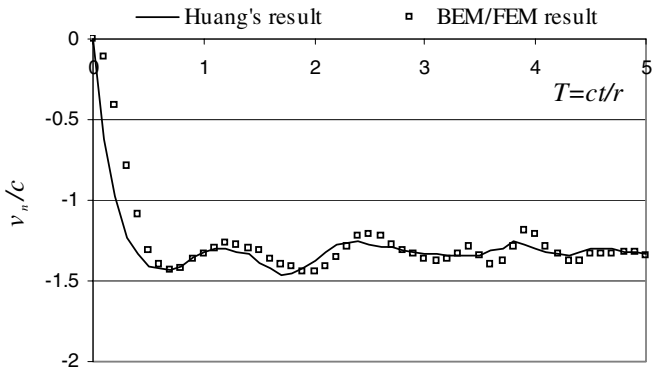

(a) $\alpha = 0$

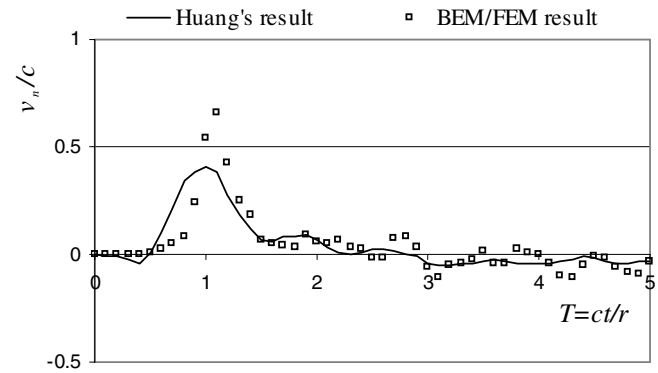

(b) $\alpha = \pi/2$

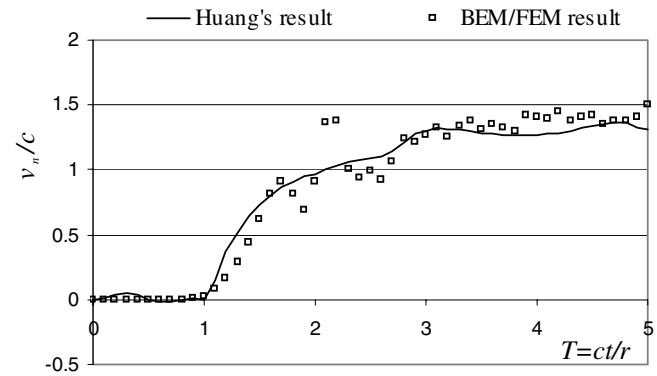

(c) $\alpha = \pi$

Figure 6 : Radical velocity of the cylinder from BEM/FEM compared with Huang's result[1986], $\Delta T = 0.14$

structure, whereas the subscript 'a' represents air. The linear θ method is used (θ=1.4). As shown in Fig. 7, 34 boundary elements are used for the structure and 16 finite elements are used for the air, the time step $\Delta t = 0.001$s. Symmetric method is used to consider the effects of the rigid ground. The explosive source is $p(x,t) = P(t)\,\delta(X - X_0)$ as shown in Fig. 7, where X_0 is the explosion point.

The dynamic pressures at different points inside the structure caused by the explosion are shown in Fig. 8. One can see that due to the opening facing to the explosion, the pressure inside the structure is greatly increased compared with that in the free air (without the structure). This means that the opening is a very important factor to be considered for designing such a structure. From Fig. 9, it can be seen that the pressure at point D outside the structure is reduced greatly.

6 Conclusions

It is ideal to model the infinite fluid/air by boundary elements and the structure by finite elements. The instability problem for the BEM algorithm can be solved by the linear θ method which is more stable than the standard algorithm [Mansur (1983)] for any time step if a bigger θ is used for a smaller time step. The coupling procedure can be used to analyze any kind of structural-acoustic interaction problem, the explosions can be of either far field or near field, and the structure can be of any shape. It can also be used to direct time-domain nonlinear analysis. Finally, 3-D structural-acoustic interaction problems can be solved in a similar way for 2-D problems.

References:

Bathe, K. J.; Wilson, E. L. (1973): Stability and accuracy analysis of direct integration methods. Earthq. Eng. Struct. Dyn., vol. 1, pp. 283-291.

Beskos, D. E. (1997): Boundary element methods in dynamic analysis: Part II (1986-1996). Appl. Mech. Rev., vol. 50, no. 3, pp.149-197.

Bettess, P.; Bettess, J. (1991): Infinite elements for dynamic problems: part 2. *Engngr. Comput.*, vol. 8, pp. 125-151.

Chen, S.; Liu Y. (1998): Application of a new composite BIE for 3-D acoustic problems. In: A. Kassab, M. Chopra, C. A. Brebbia (eds) *Boundary elements*

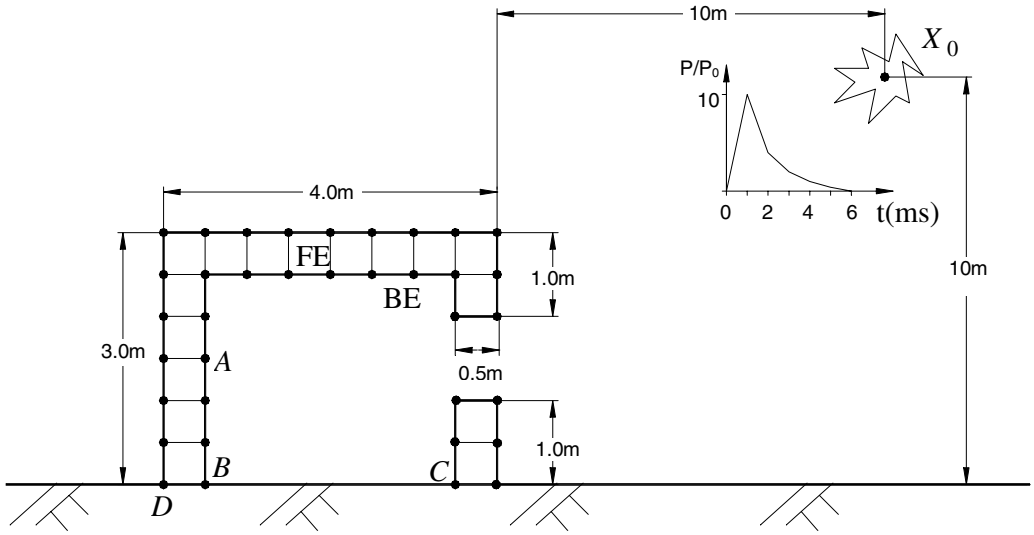

Figure 7 : The structure under an explosion

XX, Computational Mechanics Publications, Southampton and Boston, pp. 521-530.

DiMaggio, F. L.; Sandler, I. S.; Rubin, D. (1981): Uncoupling approximations in fluid-structure interaction problems with cavitation. *ASME J. of Appl. Mech.*, vol. 48, pp. 753-756.

Geers, T. L. (1969): Excitation of an elastic cylindrical shell by a transient acoustic wave. *ASME J. Appl. Mech.*, vol. 36, pp. 459-469.

Hamdan, F. H.; Dowling, P. J. (1995): Far-field fluid-structure interaction - formulation and validation. *Computers & Structures*, vol. 56, no. 6, pp. 949-958.

Huang, H. (1986): Numerical analyses of the linear interaction of pressure pulses with submerged structures. In: C. S. Smith, J. D. Clarke (eds) *Proceeding of the International Conference on Advances in Marine Structures*, Admiralty Research Establishment, Dunfermline, Elsevier Applied Science Publisher, London, 20-23 May 1986.

Mansur, W. J. (1983): A time-stepping technique to solve wave propagation problems using the boundary element method. *Ph.D. thesis*, University of Southampton.

Mindlin, R. D.; Bleich, H. H. (1952): Response of an elastic cylindrical shell to a transverse, step shock wave. *ASME J. of Appl. Mech.*, vol. 20, pp. 189-195.

O'Regan, S. D.; DiMaggio, F. L. (1990): Dynamic response of submerged shells with appendages. *ASCE J. of Eng. Mech.*, vol. 116, no. 10, pp. 2275-2292.

Pinsky, P. M.; Abbound, N. N. (1990): Transient finite element analysis of the exterior structural acoustic problem. *J. of Vibration and Acoustics*, vol. 112, pp. 245-256.

Ranlet, D.; DiMaggio, F. L.; Bleich, H. H.; Baran, M. L. (1977): Elastic response of submerged shells with internally attached structures to shock wave loading. *Computers & Structures*, vol. 7, pp. 355-364.

Soliman, M.; DiMaggio, F. L. (1983): Doubly asymptotic approximations as non-reflecting boundaries in fluid-structure interaction problems. *Computers & structures*, vol. 17, no. 2, pp. 193-204.

Tanaka, M.; Matsumoto, T.; Oida, S. (1998): Boundary element analysis of certain structural-acoustic coupling problems and its application. In: A. Kassab, M. Chopra, C. A. Brebbia (eds) *Boundary elements XX*, Computational Mechanics Publications, Southampton UK and Boston, pp. 521-530.

Yu, G.; Mansur, W. J.; Carrer, J. A. M. (1999): The linear θ method for 2-D elastodynamic BE analysis. *Computational Mechanics*, vol. 24, no. 2, pp. 82-89.

Zilliacus, S. (1983): Fluid-structure interaction and ADINA. *Computers & Structures*, vol. 17, no. 5-6, pp. 763-773.

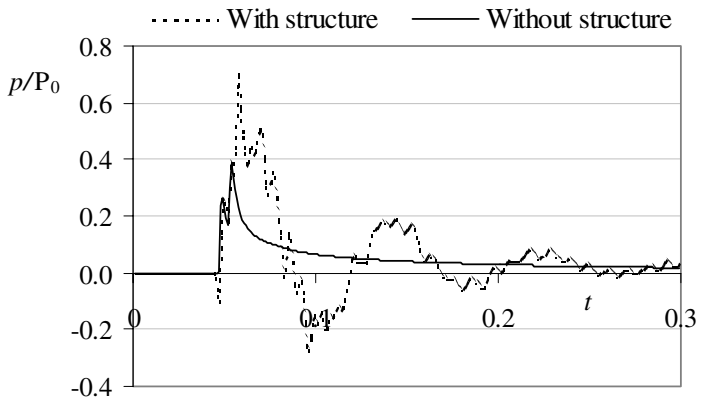

(a) Point A

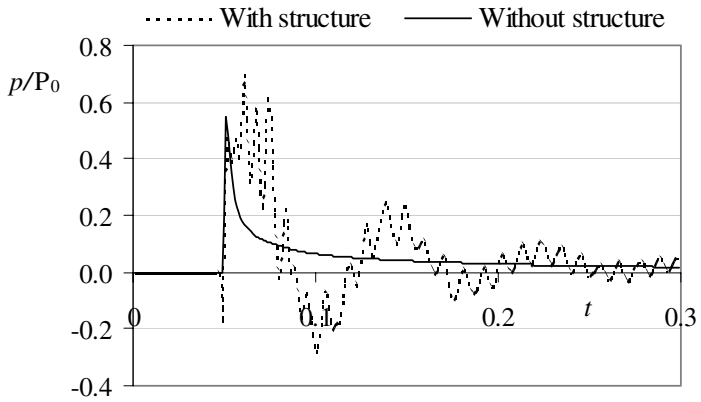

(b) Point B

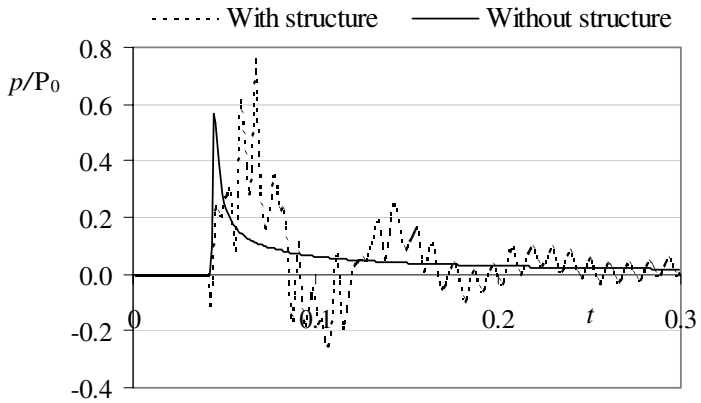

(c) Point C

Figure 8 : Pressures at different points inside the structure caused by the explosion

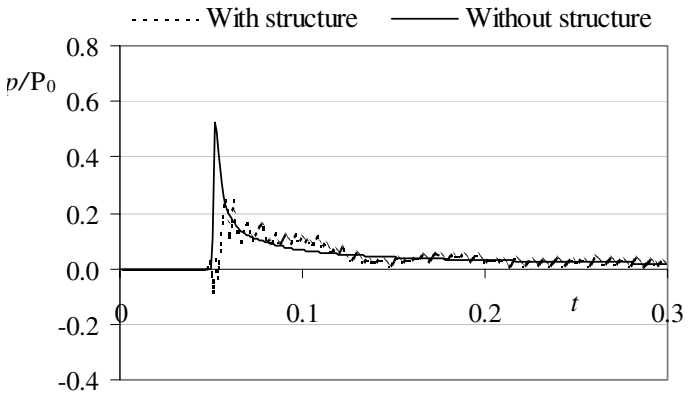

Figure 9 : Pressure at point D outside the structure caused by the explosion